



# Low Velocity Impact Response of Sandwich Beams with Composite Face-Sheets and Foam or Honeycomb Core: Analytical Modeling and Finite Element Simulation

P. Karvan, S. Feli\*

Department of Mechanical Engineering, Razi University, Kermanshah, Iran

**ABSTRACT:** In this paper, an analytical solution for the static indentation and low velocity impact response of composite sandwich beams with an orthotropic symmetric composite face-sheets and foam or honeycomb core is presented. The indentation force during impact loading consists of two regimes, one for small indentations of the top face-sheet due to bending moments and the other for larger deformation due to membrane forces. Also, the crushable core is considered a rigid-plastic foundation, and the elastic aspect is neglected. To obtain a more accurate approximation of the static indentation of the beam, both the local and global deformation of the sandwich beam are considered. The minimum potential energy method is applied for the extraction of governing equations. Furthermore, by developing a three dimensional finite element model through the ABAQUS code, the low velocity impact on composite sandwich beams with foam core is simulated. The contact force history, maximum contact force, and upper face-sheet displacement results computed by the analytical model are compared with experimental and ABAQUS simulations. A good agreement between the analytical model, finite element simulation, and experimental results, is observed.

## Review History:

Received: Oct. 28, 2021

Revised: Mar. 07, 2022

Accepted: Mar. 11, 2022

Available Online: Jun. 08, 2022

## Keywords:

Beam

Composite sandwich

Low velocity impact

Analytical model

Finite element simulation

## 1- Introduction

The use of composite sandwich structures expanded as they can provide better performance due to their strength, stiffness, and resistance to impacts. Being lightweight is also a crucial feature for structures in industries such as aerospace, automotive, and marine; this quality could be fulfilled by using composite sandwich structures. The US Navy, for instance, benefits from honeycomb sandwich structures in bulkheads, deck houses, and helicopter hangars to reduce their weight; other applicants of these structures are in the body of sailboats and racing craft. Furthermore, the use of sandwich structures in infrastructure rehabilitation projects such as bridge decks in civil engineering indicates the wide range of its usage [1].

Since composite sandwich structures might undergo different kinds of local loadings during their longevity, like tool dropping, bird striking, and so on, a comprehensive perception of their behavior and failure is vital for a more dependable design. Low velocity impacts are dangerous for a composite sandwich structure as it is difficult to observe the damage; they could also substantially reduce the capacity of the load that the structures could be endurance [2, 3]. Therefore, understanding and predicting their behavior and the effect of low velocity impact on the performance of structures is necessary.

In addition to some thorough reviews in this area [4-6], there are considerable researches which have intended to approach the subject in experimental, analytical, and numerical ways with the aim of detecting the deformation and failures of composite sandwich panels under impacts. There are many experimental pieces of research in this case [7-10]; Wu and Sun [11] experimentally studied failures and damages in a sandwich panel with foam core and graphic /epoxy face-sheets due to low velocity impacts. According to their study, matrix cracking and delamination in composite and cracking in the foam were the paramount modes of failure.

Anderson and Madenci [12] presented an experimental investigation of the damage in sandwich panels with both foam and honeycomb core under the low-velocity impact. They indicated that structures with a higher density of foam and thicker face sheets need more energy to generate the damage, but the residual indentation is similar to those with lower density foam.

A considerable number of numerical studies have been conducted on composite sandwich panels [13-15]. Ivañez and Sanchez-Saez [16], presented a numerical model for a composite sandwich beam with a honeycomb core subjected to a low velocity impact with different impact energies. She concluded that the core was responsible for the absorption of energy in the lowest velocities, while the participation of face sheets in higher velocities was more significant. Also, through a Finite element (FE) simulation with ABAQUS/

\*Corresponding author's email: Felisaeid@razi.ac.ir



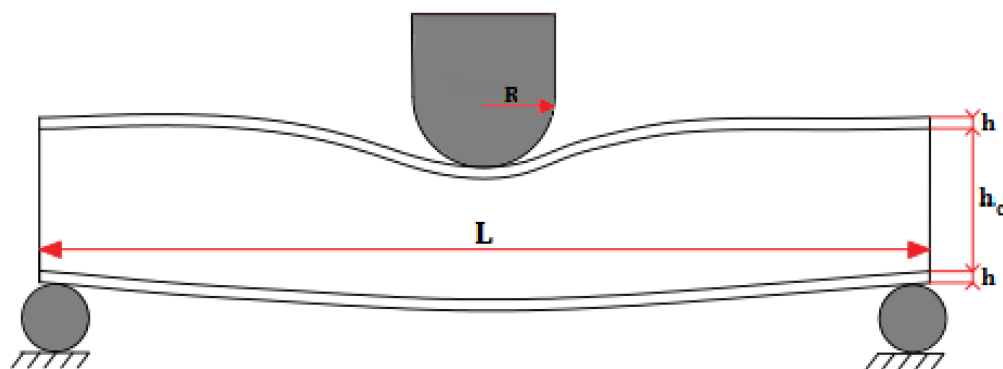


**Fig. 1. Scheme of a sandwich composite beam subjected to low velocity impact.**

Explicit code, Ivañez et al [17] indicated that the core collapse under the impact area is more possible than failure in the top face-sheet.

Given that pursuing a numerical study according to its complexity requires a considerable effort, there has been a growing tendency toward adopting analytical procedures. Most impact analyses are based on common spring-mass models, like one degree of freedom [18], or two degrees of freedom [19, 20], and contact laws, such as Hertz's law, Mayer's law [21, 22], Hasebe and Sun's law [23], Choi's linear contact equation [24].

While the overwhelming majority of studies have concentrated on analyzing low velocity impact on composite sandwich panels [15, 25, 26] there are fewer research projects on sandwich beams that are used in different structures such as wind turbine blades. Frostig [27-29] investigated different aspects of sandwich beams by considering the bending behavior, buckling of sandwich beams, and their free vibration. The face sheets were modeled by the higher order plate theory. Localized indentation of a sandwich beam was investigated by Xie et al [30] and Navaro et al [31]. This solution was based on an approximation deformation profile for composite sandwich beams subjected to either a flat or a spherical indenter. By using minimum potential energy, an expression for indentation force was presented. Dobyns [32] tried to approach the behavior of a composite sandwich beam by considering different methods for core behavior. They presented two models for the elastic behavior of a core, with the Vlasov's model showing a better agreement than Winkler's model. A new analytical approach was presented by Ivañez et al. [2] which was based on Zhongyou's model. One of the differences between the two models was that Ivañez simplified the approach by replacing the spherical indenter with a flat one.

The modified solution in this paper (i.e. the exact deformation profile for a spherical nose indenter) has been considered. Another new facet of this study is the material behavior of the foam core, which is considered as plastic behavior.

This paper presents a modified analytical solution for

the contact force history and top face-sheets deflection of sandwich composite beams under low velocity impact. The indentation force consists of two regimes, one for small indentations of the top face-sheet due to bending moments and the other for larger deformation due to membrane forces. The previous analytical models only considered large indentations. In the current study, the original deformation profile for the top face sheet is used. In addition, only the plastic behavior of the core is considered. The minimum potential energy is applied for driving the indentation force and the contact force is determined by using the discrete mass-spring model. The results are validated in the light of two independent experimental works and an analytical model. In addition, the FE simulation with ABAQUS/Explicit code is provided for comparison with the analytical model.

## 2- Analytical Solution

### 2- 1- Static indentation

The composite sandwich beam with the same top and bottom laminated face-sheets of thickness  $h$  is illustrated in Fig. 1. The core has a thickness of  $h_c$  in the middle and is made of foam or honeycomb, while the beam has a width of  $b$  and a length of  $L$  with the simply supported boundary conditions also, the shape of a hemispherical-nose cylinder is considered for impactor.

In this paper, to obtain a more accurate approximation of the static indentation of the beam, both the local and global deformation of the sandwich beam are considered.

#### 2- 1- 1- Local deformation

Most of the previous studies have used Hertz's contact law for determining the local deformation; this law would be inappropriate if the effects of core crushing and transverse deflections of the top sheet were considered.

The core could experience two modes of deformation depending on the local indentation. For a short period of impact, while the deformation reaches a specific amount, the core would be in an elastic mode, and then it changes to a rigid- plastic foundation. The deformation from the elastic to plastic mode is low, so the elastic mode of deformation

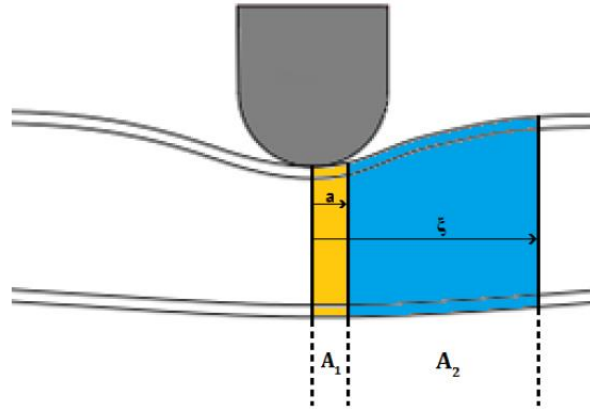


Fig. 2. Contact area between the impactor and top face-sheet

is negligible; however, Abrate [4, 5] and Navarro et al. [31] presented expressions for this period of time. Thus, the structure in this paper is considered as a beam on a rigid-plastic foundation until the local indentation reaches the height of the face sheet. At this time, it is considered as a membrane resting on a perfectly plastic foundation.

2- 1- 2- Beam Resting on a perfectly plastic foundation

The method used for driving the relationship between the indentation force and local indentation of the top face sheet is based on minimizing the potential energy of the composite beam. The potential energy  $\Pi$  is:

$$\Pi = U + D - V \tag{1}$$

Where  $U$ ,  $D$  and  $V$  are the strain energy due to bending, the work due to core crushing, and the work done by indentation force, respectively.

The displacement profile of the face sheet is assumed as:

$$w(x) = \begin{cases} \delta - \frac{x^2}{2R} \\ (\delta - \frac{a^2}{2R}) \left[ 1 - \frac{(x-a)^2}{(\xi-a)^2} \right]^2 \end{cases} \tag{2}$$

Where  $a$  is the radius of contact area between impactor face-sheet, and  $\xi$  represents the radius of total deformation area,  $R$  and  $\delta$  are the impactor radius and indentation, respectively.

The strain energy due to the bending  $U$  of cross-ply laminate is expressed as [3, 25]:

$$U = \frac{1}{2} \int_A \left[ D_{11} \left( \frac{\partial^2 w}{\partial x^2} \right)^2 + D_{22} \left( \frac{\partial^2 w}{\partial y^2} \right)^2 + 2D_{12} \left( \frac{\partial^2 w}{\partial x^2} \right) \left( \frac{\partial^2 w}{\partial y^2} \right) + 4D_{66} \left( \frac{\partial^2 w}{\partial x \partial y} \right)^2 \right] dA \tag{3}$$

The work due to core crushing  $D$  is equal to:

$$D = \int_{A_1} q w_{(x)} dA + \int_{A_2} q w_{(x)} dA \tag{4}$$

Finally, the work done by the indentation force is given by:

$$V = \int_{A_1} \frac{P}{2ab} w_{(x)} dA \tag{5}$$

As shown in Fig. 2, the region of beam experience impact has been divided into two areas; the area exactly under the impactor, where the face-sheet and impactor are in direct contact (called  $A_1$ ), and the region that is not in direct contact with impactor but experiences the effect of the impact which is (known as  $A_2$ ). Where:

$$\int_{A_1} dA = 2 \int_0^a \int_0^b dx dx \tag{6}$$

$$\int_{A_2} dA = 2 \int_0^{\xi} \int_a^b dx dx \tag{7}$$

$$\int_A dA = \int_{A_1} dA + \int_{A_2} dA$$

By using Eqs. (6) and (7) and substituting Eq. (2) into (3), the following expression for strain energy would be derived:

$$U = \frac{D_{11}}{2} \left[ \frac{2ab}{R^2} + \frac{128ab}{5(\xi - a)^3} \left( \delta - \frac{a^2}{2R} \right)^2 \right] \tag{8}$$

By the same sequence, work due to core crushing and indentation force given by:

$$D = 2bq \left[ \left( a\delta - \frac{a^3}{6R} + \frac{8}{15} \left( \delta - \frac{a^2}{2R} \right)^2 (\xi - a) \right) \right] \tag{9}$$

$$V = P \left( \delta - \frac{a^2}{2R} \right) \tag{10}$$

Therefore, the total potential energy is equal to:

$$\begin{aligned} \Pi = & \frac{D_{11}}{2} \left[ \frac{2ab}{R^2} + \frac{128ab}{5(\xi - a)^3} \left( \delta - \frac{a^2}{2R} \right)^2 \right] + \\ & 2bq \left[ \left( a\delta - \frac{a^3}{6R} \right) + \frac{8}{15} \left( \delta - \frac{a^2}{2R} \right) (\xi - a) \right] - \\ & P \left( \delta - \frac{a^2}{2R} \right) \end{aligned} \tag{11}$$

In order to obtain  $P$  from the previous equation, Eq. (11) is minimized with respect to  $\delta$  :

$$P = \frac{128bD_{11}}{5(\xi - a)^3} \left( \delta - \frac{a^2}{2R} \right)^2 + 2bq \left[ a + \frac{8}{15} (\xi - a) \right] \tag{12}$$

For eliminating  $\xi$  and presenting the indentation force in terms of local deformation, Eq. (12) is minimized with

respect to  $\xi$  :

$$\xi - a = \sqrt[4]{\frac{72D_{11}}{q} \left( \delta - \frac{a^2}{2R} \right)} \tag{13}$$

Therefore:

$$P = 2abq + \left[ \frac{512bD_{11}}{5^4 \sqrt{\left( \frac{512bD_{11}}{q} \right)^3}} \right] \left( \delta - \frac{a^2}{2R} \right)^{\frac{1}{4}} \tag{14}$$

### 2- 1- 3- Membrane resting on a perfectly plastic foundation

In this condition, the displacement profile is assumed to have a quadratic form [30, 31]:

$$w(x) = \begin{cases} \delta - \frac{x^2}{2R} \\ \left( \delta - \frac{a^2}{2R} \right) \left[ 1 - \frac{(x - a)}{(\xi - a)} \right]^2 \end{cases} \tag{15}$$

The work due to crushing core and indentation force can be derived as:

$$D = 2bq \left[ \left( a\delta - \frac{a^3}{6R} \right) + \frac{(\xi - a)}{3} \left( \delta - \frac{a^2}{2R} \right) \right] \tag{16}$$

$$V = P \left( \delta - \frac{a^2}{2R} \right) \tag{17}$$

Also, the elastic strain energy is given by [25]:

$$U = \frac{1}{8} \int_A \left[ A_{11} \left( \frac{\partial w}{\partial x} \right)^4 + A_{22} \left( \frac{\partial w}{\partial y} \right)^4 + (2A_{12} + 2A_{66}) \left( \frac{\partial w}{\partial x} \right)^2 \left( \frac{\partial^2 w}{\partial y^2} \right) \right] dA \tag{18}$$

Considering Eqs. (6 ) and (7) and substituting the displacement field in Eq. (18), the expression for the elastic strain energy would be derived as:

$$U = \frac{A_{11}}{2} \left[ \frac{2a^5b}{5R^4} + \frac{32b}{5(\xi - a)^3} \left( \delta - \frac{a^2}{2R} \right)^4 \right] \quad (19)$$

Therefore, the potential energy in this condition is calculated by substituting Eqs. (16), (17) and (19) into Eq. (1):

$$\begin{aligned} \Pi = & \frac{A_{11}}{8} \left[ \frac{2ab^5}{5R^4} + \frac{32b}{5(\xi - a)^3} \left( \delta - \frac{a^2}{2R} \right)^4 \right] + \\ & 2bq \left[ \left( a\delta - \frac{a^3}{6R} \right) + \frac{(\xi - a)}{3} \left( \delta - \frac{a^2}{2R} \right) \right] - \\ & P \left( \delta - \frac{a^2}{2R} \right) \end{aligned} \quad (20)$$

By minimizing Eq. (20); with respect to  $\delta$  and  $\xi$ , the expression for indentation force in terms of local indentation is derived as:

$$P = 2abq + \left[ \frac{64bA_{11}}{5^4 \sqrt{\left( \frac{72A_{11}}{5q} \right)^3}} \right] \left( \delta - \frac{a^2}{2R} \right)^{\frac{3}{4}} \quad (21)$$

In Eqs. (14) and (21), the indentation force is a function of local indentation  $\delta$  and contact radius  $a$ . For eliminating contact radius, the above equations must be minimized with respect to  $a$  which is difficult. Another approach used by Turk and Hoo Fat [25] is considering  $a = 0.4R$ . The difference between the two solutions is 3%.

#### 2- 1- 4- Global deformation

The sandwich beam has two different deformations during impact, one is local deformation  $\delta$ , which is the top face sheet's local indentation during core crushing; and the second is global deformation  $\Delta$ , which consists of core shearing  $\Delta_s$  and face-sheet bending deformation  $\Delta_b$ :

$$\Delta = \Delta_s + \Delta_b \quad (22)$$

The bending deformation of a simply supported beam is given by:

$$\Delta_b = \frac{PL^3}{48(EI)_{eq}} \quad (23)$$

And core shear deformation is expressed as:

$$\Delta_s = \frac{PL}{4(GA)_{eq}} \quad (24)$$

Where the equivalent flexural rigidity and shear rigidity are equal to [24]:

$$(EI)_{eq} = \frac{E_{11}bh(h_c + h)^2}{2} + \frac{E_{11}bh^3}{6} + \frac{E_cbh_c^3}{12} \quad (25)$$

$$(GA)_{eq} = \frac{b(h_c + h)^2 G_c}{h_c} \quad (26)$$

By substituting Eqs. (23) and (24) into Eq. (22), the global deformation is given by:

$$\Delta = \frac{PL^3}{48(EI)_{eq}} + \frac{PL^3}{4(GA)_{eq}} \quad (27)$$

And the global stiffness of the sandwich beam could be written as:

$$K_g = \frac{P}{\Delta} \quad (28)$$

#### 2- 2- Low velocity impact

In this study, Hoo Fatt's two degrees of freedom model was used to indicate the contact force history and top face sheet deflection. In this discrete system,  $k_g$  is the global stiffness,  $k_f$  is the top face-sheet stiffness, and  $m_f, m_s$  are equivalent effective masses of face-sheet and sandwich beam, respectively.  $M_0$  is the mass of the impactor (Fig. 3).

Equations of motion for this system could be described as [2]:

$$(M_0 + m_f)(\ddot{\Delta} + \ddot{\delta}) + P_{i(\delta)} + Q_d = 0 \quad (29)$$

$$P_{i(\delta)} + Q_d = m_s \ddot{\Delta} + K_g \Delta \quad (30)$$

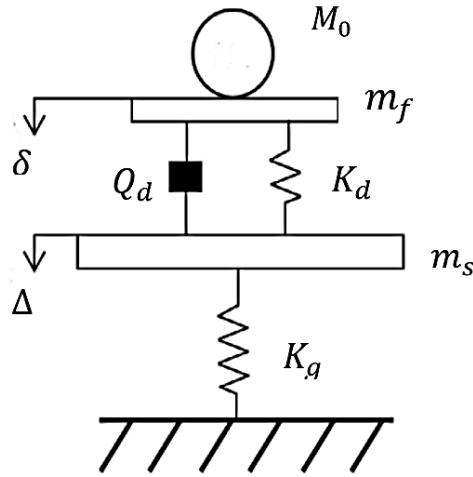


Fig. 3. Discrete Dynamic two degrees of freedom system [1, 2]

And the initial conditions are:

$$\Delta_{(0)} = 0, \dot{\Delta}_{(0)} = V_0, \delta_{(0)} = 0, \dot{\delta}_{(0)} = 0 \quad (31)$$

Where  $Q_d$  is the dynamic resistance of the core during crushing:

$$Q_d = 2abq_d \quad (32)$$

And  $P_{i(\delta)}$  is the dynamic indentation force based on the local indentation; it would be either:

$$P_{1(\delta)} = 2abq + \left[ \frac{512bD_{11}}{5.4\sqrt{\left(\frac{72D_{11}}{q_d}\right)^3}} \right] \left(\delta - \frac{a^2}{2R}\right)^{\frac{1}{4}} \quad (33)$$

For small local indentations and:

$$P_{2(\delta)} = 2abq + \left[ \frac{64bA_{11}}{5.4\sqrt{\left(\frac{72A_{11}}{5q_d}\right)^3}} \right] \left(\delta - \frac{a^2}{2R}\right)^{\frac{3}{4}} \quad (34)$$

For indentations further than the top face-sheet's height.

By solving the system of Eqs. (29) and (30) numerically and calculating global deformation  $\Delta$ , and local indentation  $\delta$ , the top face-sheet deflection history can be defined as:

$$w_t = \Delta + \delta \quad (35)$$

And the contact force in terms of time can be drawn as:

$$F_{(t)} = -M_0(\ddot{\Delta} + \ddot{\delta}) \quad (36)$$

### 2- 3- Effective masses:

For small indentation, for determining the effective mass of the top face-sheet in each regime, the velocity profile according to Eq. (2) is given by:

$$w(x) = \begin{cases} \dot{\delta} \\ \dot{\delta} \cdot \left[ 1 - \frac{(x-a)^2}{(\xi-a)^2} \right]^2 \end{cases} \quad (37)$$

Therefore, the kinetic energy can be approximated as:

$$KE \approx bh\rho_f\dot{\delta}^2 \left[ a + \frac{128(\xi-a)}{315} \right] \quad (38)$$

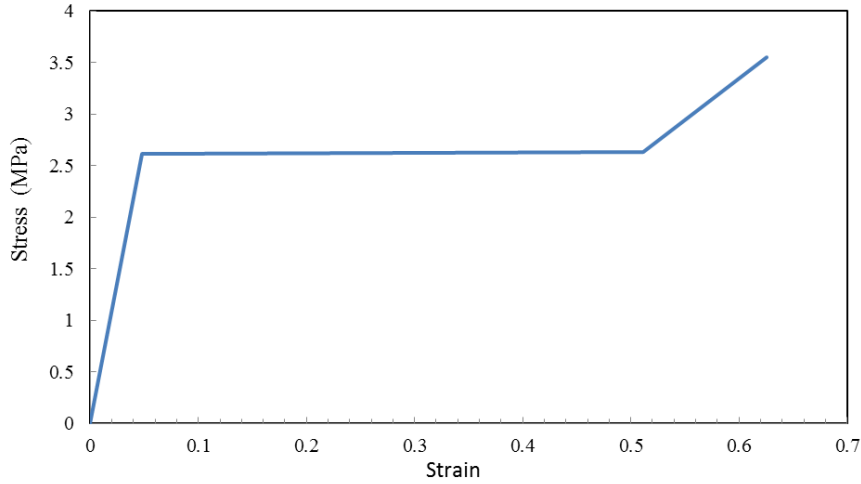


**Fig. 4. Nominal stress- strain curve of a compression test on PVC foam [16]**

The kinetic energy of the top face-sheet with respect to effective mass is equal to:

$$KE = \frac{1}{2} m_f \dot{\delta}^2 \quad (39)$$

From Eqs. (38) and (39), the effective mass for the small deformation is expressed as:

$$m_f = 2bh\rho_f \left[ a + \frac{128(\xi - a)}{315} \right] \quad (40)$$

The same sequence is utilized to derive the effective mass of the top face sheet at large deformations. The displacement profile in Eq. (15) is taken into account to derive the velocity profile; thus, the effective mass would be:

$$m_s = 2bh\rho_f \left[ a + \frac{(\xi - a)}{5} \right] \quad (41)$$

According to Iváñez et al.'s study [2], the deformation zone  $\xi$  can be approximated as the quarter of the beam's length.

By considering the displacement profile of the sandwich beam under a central load the same as the profile in Dobyns's research [36], the  $KE$  is given as:

$$KE \approx \frac{4}{15} \rho_s b (h_c + 2h) L \dot{\Delta}^2 \quad (42)$$

The  $KE$  with respect to the effective mass of the sandwich beam is also:

$$KE = \frac{1}{2} m_s \dot{\Delta}^2 \quad (43)$$

Therefore, the effective mass of the sandwich beam has the following expression:

$$m_s = \frac{8}{15} \rho_s b (h_c + 2h) L \quad (44)$$

### 3- Numerical Modeling

An ABAQUS/Explicit code [33] is used to develop a numerical model to analyze the low velocity impact of composite sandwich beam with foam core.

Each face-sheet is made from 5 plies cross-ply E-glass fibers and polyester resin with the following angles [0/90/0/90/0]. The elastic geometrical and mechanical properties of the composite, core, and impactor are listed in Table 1.

The core is considered as a crushable foam with elastic and plastic behavior. The elasticity and plasticity behavior could be determined by the strain-stress curve in compression presented in Fig. 4. From the stress-strain curve presented in Fig. 4, it can be observed that when the stress reaches the yield stress, the foam, which is made of cells, begins to collapse. In the plastic yielding plateau, however, while the strain increases, the stress stays almost the same. By continuing the load, densification of the core material starts, and almost all the cell walls crush with each other, and the last section of the stress-strain curve is happening [17].

**Table 1. Geometrical and material properties of the impactor and composite sandwich beam with foam core [17]**

| <b>Face sheets: E-glass fibers and polyester resin AROPOL FS6902</b> |                                    |
|--|------------------------------------|
| Beam's length  | $L = 480\text{mm}$                 |
| Beam's width   | $b = 50\text{mm}$                  |
| Face sheet's height  | $h = 3\text{mm}$                   |
| Face sheet's density   | $\rho_f = 1800\text{kg/m}^3$       |
| <b>Ply features</b>  |                                    |
| Longitudinal stiffness   | $E_{11} = 10.1\text{GPa}$          |
| Transverse stiffness   | $E_{22} = 10.1\text{GPa}$          |
| Poisson's ratio  | $\nu_{12} = 0.16$                  |
| In- plane shear modulus  | $G_{12} = 3.1\text{GPa}$           |
| Tensile strength   | $X_T = Y_T = 367.4\text{MPa}$      |
| Compressive strength   | $X_C = Y_C = 367.4\text{MPa}$      |
| Transverse shear strength  | $S_{13} = S_{23} = 34.3\text{MPa}$ |
| <b>Core: PVC foam</b>  |                                    |
| Core's height  | $h_c = 30\text{mm}$                |
| Core's density   | $\rho_c = 100\text{kg/m}^3$        |
|  | Core features                      |
| Young's Modulus  | $E_C = 87\text{MPa}$               |
| Poisson's ratio  | $\nu_C = 0.3$                      |
| <b>Striker: Hemispherical nose steel cylinder</b>                    |                                    |
| Mass   | $M_0 = 5.88\text{kg}$              |
| Radius   | $R = 10\text{mm}$                  |
| Velocity   | $V_0 = 2.5 - 4 \text{ m/s}$        |
|  | Striker feature                    |
| Young's Module   | $E_0 = 210\text{GPa}$              |
| Poisson's ratio  | $\nu_0 = 0.3$                      |

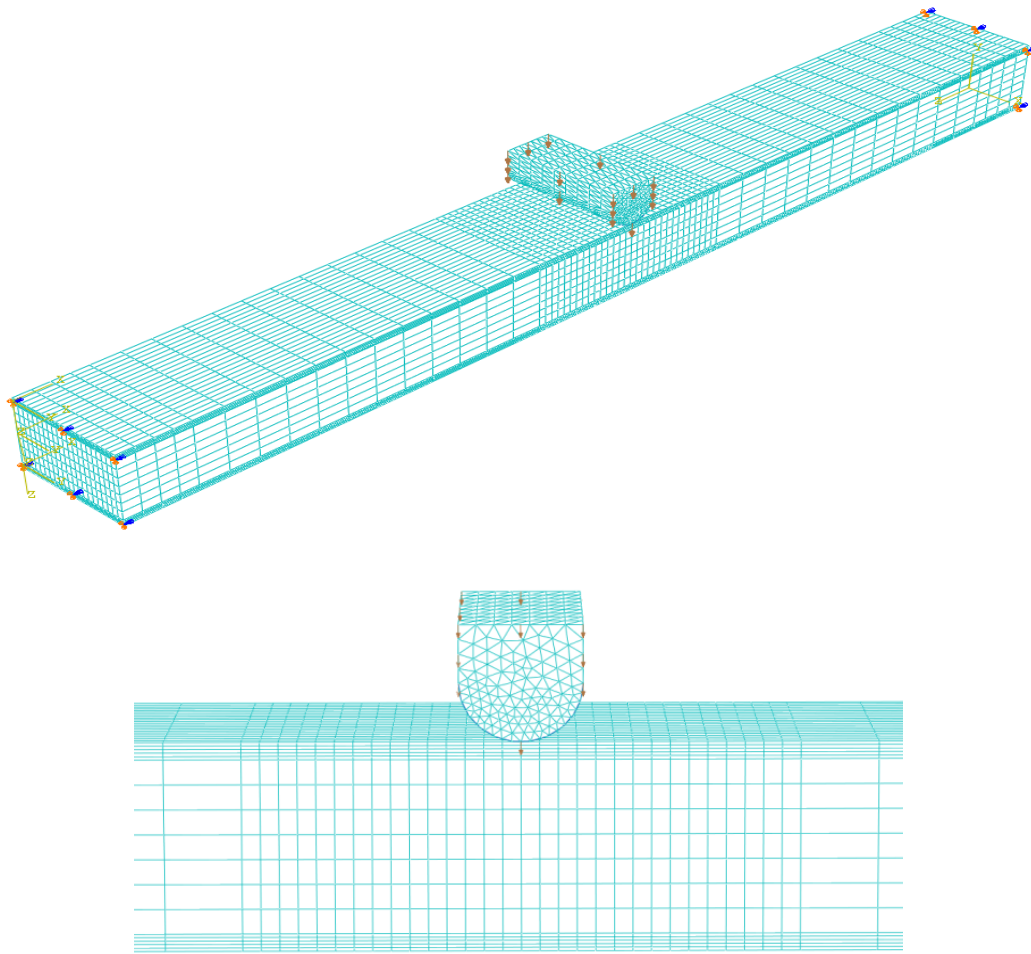


**Fig. 5. FE simulation in ABAQUS code**

The sandwich beam in this study has simply supported boundary conditions, the vertical displacements restricted at two ends of the beam. The mesh scheme for the composite sandwich beam and impactor is shown in Fig. 5.

In order to have a more accurate estimation of the number of elements, a comparison between this factor and maximum contact force is conducted. In this comparison, miscellaneous scenarios, each of which embodies a unique number of elements disseminated differently throughout the beam, are taken into consideration. Fig. 6 indicates that for the number of elements more than 25000, the maximum contact force remains stable (around 3550 N).

Two composite face sheets are merged to the foam core by using TIE CONSTRAINT and the contact between the impactor and the whole sandwich beam is a frictionless surface-to-surface contact. Figs. 7 and 8 demonstrate the process of impact on a composite sandwich beam with a foam core and contour of deflection of the top face-sheet at the same impact energy and different impact mass and velocity.

#### 4- Results and Discussion

In this section, the contact force history, maximum contact force, and deflection of the composite sandwich beam predicted by the new model are compared to the results of available experimental studies [17] and the analytical model [2]. Moreover, the contact force history computed by ABAQUS, and FE simulations, are compared with the analytical model and Ivañez et. al's [17] simulations.

Two configurations of composite sandwich beams are considered in this paper. The geometrical and mechanical properties of impactor, face-sheets, and cores are listed in Tables 1 and 2.

The first comparison is based on a composite sandwich beam with foam core. The characteristics of sandwich beam and impactor are based on Table 1. In Fig. 9, the contact-force history predicted by the new model has been compared with experimental results [17]. A good agreement is observed between experimental results and the new analytical model. The differences between the results of experimental studies

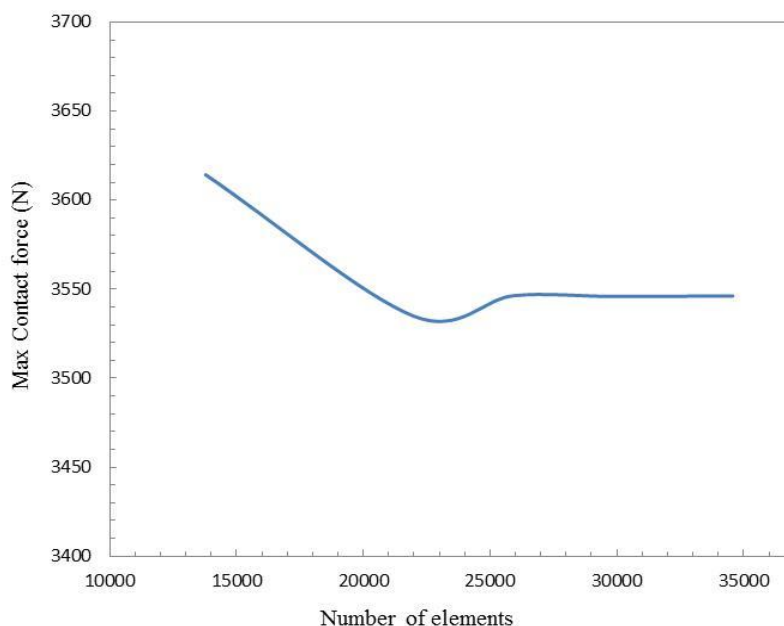


**Fig. 6. Maximum contact force versus number of elements**

and those of the new model for computing contact duration and maximum contact force are about 0.35% and 7.5%, respectively. Oscillations observed in the contact force are determined based on numerical simulation due to the reciprocation of the stress wave in the numerical simulation, which is not considered in the analytical model.

In Fig. 10, the maximum contact force determined by the new analytical model has been compared with experimental results [17] at impact energy 25 to 75J. The difference between the experimental and new model results is less than 10%. At impact energies lower than 55J, the analytical solution has a significant agreement with experimental results and the difference is less than 6.55%. However, for higher impact energies, the difference between the experimental results and those of the new model increases; in the new model presented in this paper, the failure and damage in composite face-sheets and core are ignored; however, the stiffness of sandwich beam with the initiation of damage decreases, which is neglected in the new analytical model.

In Fig. 11, the maximum deflection of the upper face-sheet versus impact energy is shown. The analytical solution in this comparison shows a reasonable agreement with the experimental results [17] for the prediction of maximum deflection of the composite sandwich beam. Also, with trebling the impact energy, the maximum deflection increases by double.

In the second comparison, the low velocity impact on sandwich composite beam with honeycomb core is investigated. The characteristics of the sandwich honeycomb beam and impactor are listed in Table 2. The comparison was made with three distinguished velocities including, 2.04, 2.62, and 2.77 m/s.

In Fig. 12, the contact force history computed by the new model was compared with experiment results [16] and Ivanez's model [16]. It is clear that the contact force history computed by the new model has better consistency with experimental results than Ivanez's model [16].

Also, in Tables 3 and 4, the maximum contact force and contact duration determined by the new model are compared by experimental results [16], respectively. The maximum difference between contact duration and maximum contact force are 3.22% and 8.23% respectively. Additionally, by increasing impact energy, as expected, the maximum contact force increases, and the contact duration is constant, approximately.

In the next part, the comparison between the FE simulations with the ABAQUS code and Ivanez numerical model [17] for a composite sandwich beam with foam core is described. The impactor and sandwich beam specifications are presented in Table 1. The comparison is aimed at validating the numerical solution in this paper. Fig. 13 presents a comparison between the results of contact force history computed by the ABAQUS simulation and Ivanez's numerical model [17].

In this figure, the thicknesses of composite skins are equal to 2 mm. The composite sandwich beam was struck by an 8kg mass and 20mm diameter striker. A good agreement is observed between the contact force history in the ABAQUS simulation and Ivanez's numerical model [17]. The deviations for maximum contact force and contact duration are almost 6.85% and 2.04%, respectively. In the new FE simulation, presented in this paper, failure and damage of the composite faces-sheet and foam core and the strain rate effects were neglected. The composite face-sheet and the core are made of E-glass fibers and polyester resin AROPOL FS6902 and PVC

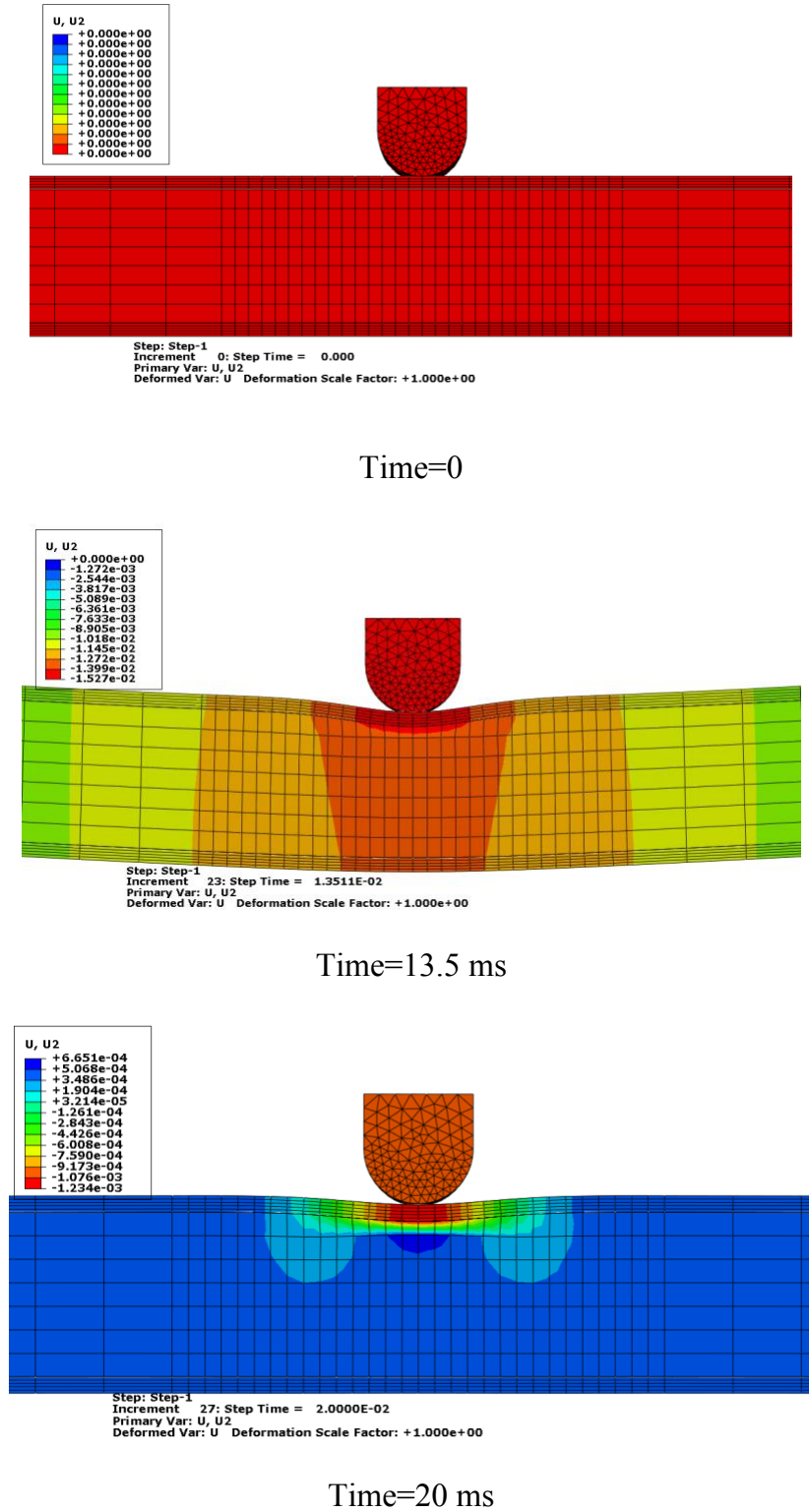
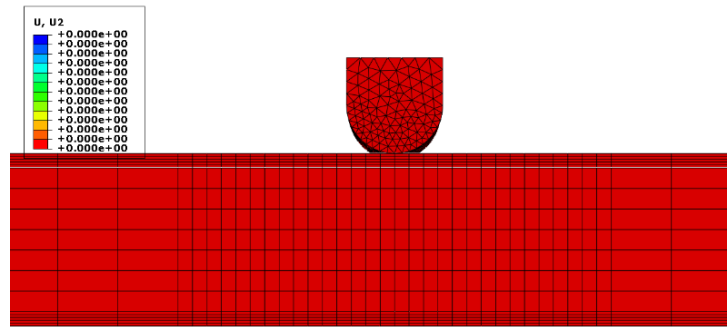
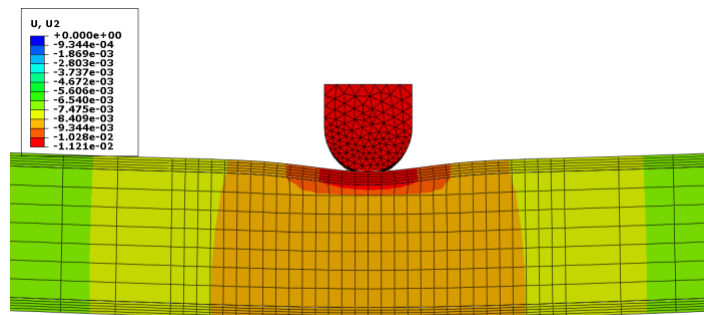


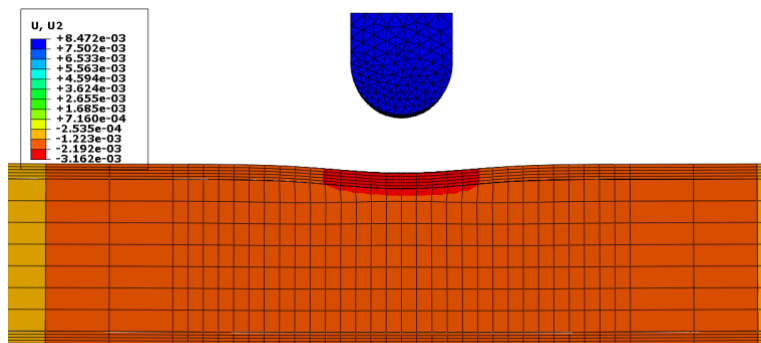
Fig. 7. The process of impact on foam based sandwich composite beam. Impact velocity: 3m/s, Impactor mass: 8kg



Time=0



Time=13.5 ms



Time=20.3ms

Fig. 8. The process of impact on foam based sandwich composite beam. Impact velocity: 3.5 m/s, impactor mass: 5.88 kg

**Table 2. Geometrical and material properties of the impactor and composite sandwich beam with honeycomb core [16]**

| <b>Faces-sheet: Carbon fiber and epoxy resin (AS4-8552)</b> |                                      |
|---|--------------------------------------|
| Beam's length   | $L = 480\text{mm}$                   |
| Beam's width  | $b = 50\text{mm}$                    |
| Face sheet's height   | $h = 2\text{mm}$                     |
| Face sheet's density  | $\rho_f = 1600\text{kg/m}^3$         |
| <b>Ply features</b>   |                                      |
| Longitudinal stiffness                                      | $E_{11} = 68.9\text{GPa}$            |
| Transverse stiffness  | $E_{22} = 68.9\text{GPa}$            |
| Poisson's ratio   | $\nu_{12} = 0.22$                    |
| In- plane shear modulus                                     | $G_{12} = 9\text{GPa}$               |
| <b>Core: 3003 alloy hexagonal aluminum honeycomb</b>        |                                      |
| Core's height   | $h_c = 20\text{mm}$                  |
| Core's density  | $\rho_C = 77\text{kg/m}^3$           |
| Core features   |                                      |
| In- plane shear modulus                                     | $G_C = 144\text{MPa}$                |
| <b>Striker: Hemispherical nose steel cylinder</b>           |                                      |
| Mass  | $M_0 = 4\text{kg}$                   |
| Radius  | $R = 10\text{mm}$                    |
| Velocity  | $V_0 = 2.04, 2.62, 2.77 \text{ m/s}$ |
| <b>Striker feature</b>                                      |                                      |
| Young's Module  | $E_0 = 210\text{GPa}$                |
| Poisson's ratio   | $\nu_0 = 0.3$                        |

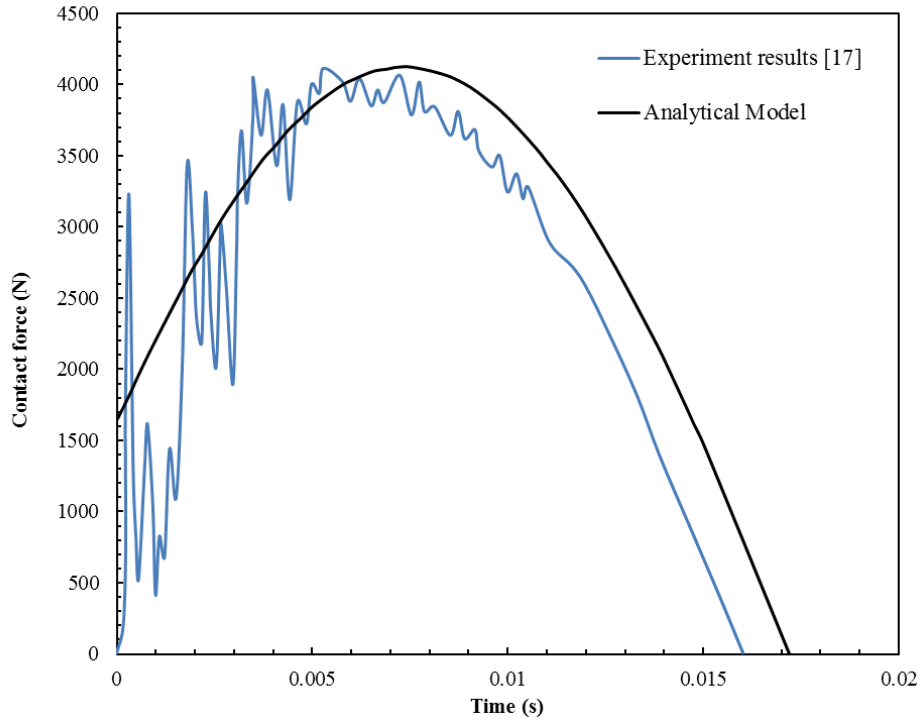


**Fig. 9. Experimental and analytical contact force history in composite sandwich beam with FOAM core. (Impact velocity: 3m/s, impactor mass: 8 kg)**

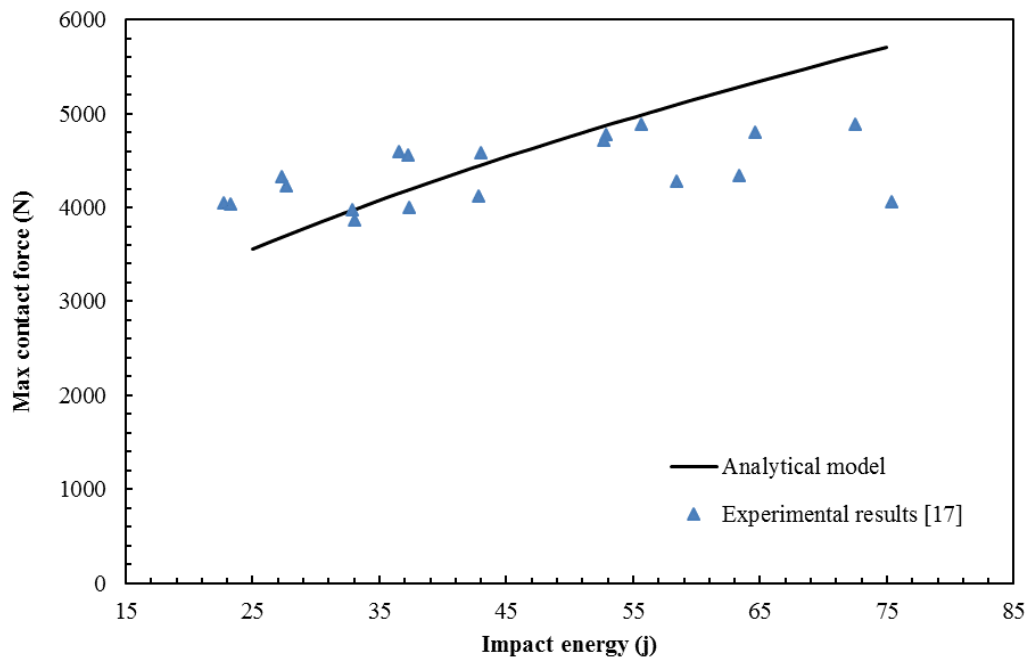


**Fig. 10. Experimental and analytical maximum contact force of composite sandwich beam with FOAM core in various impact energies.**

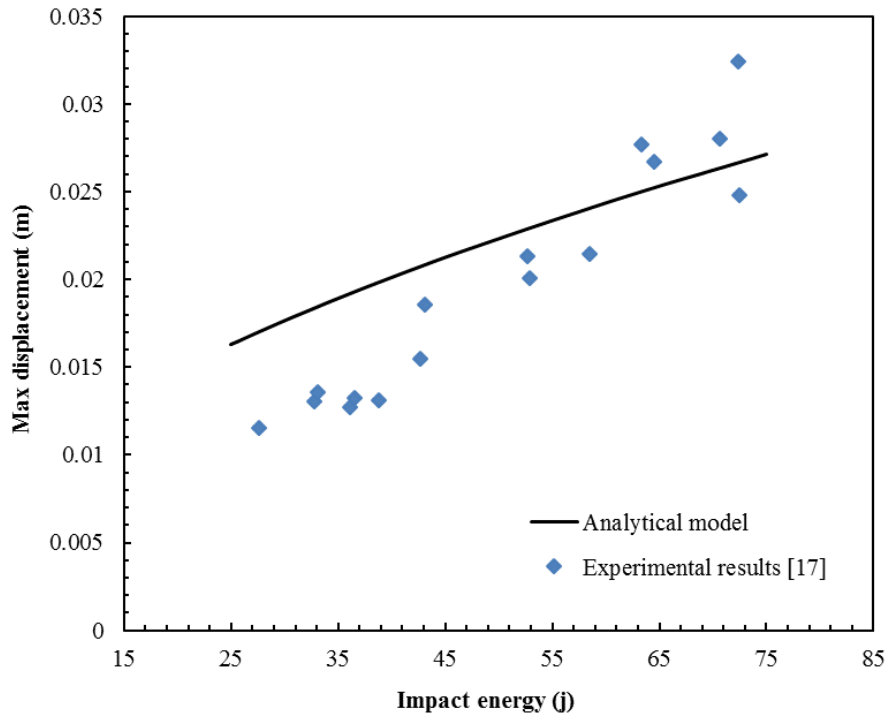
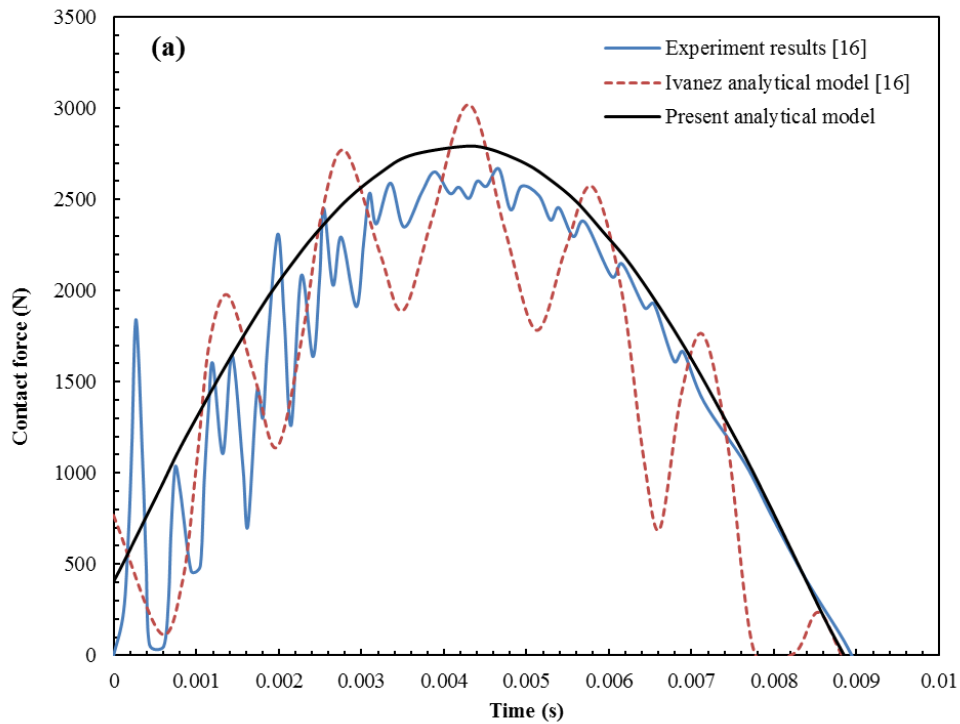
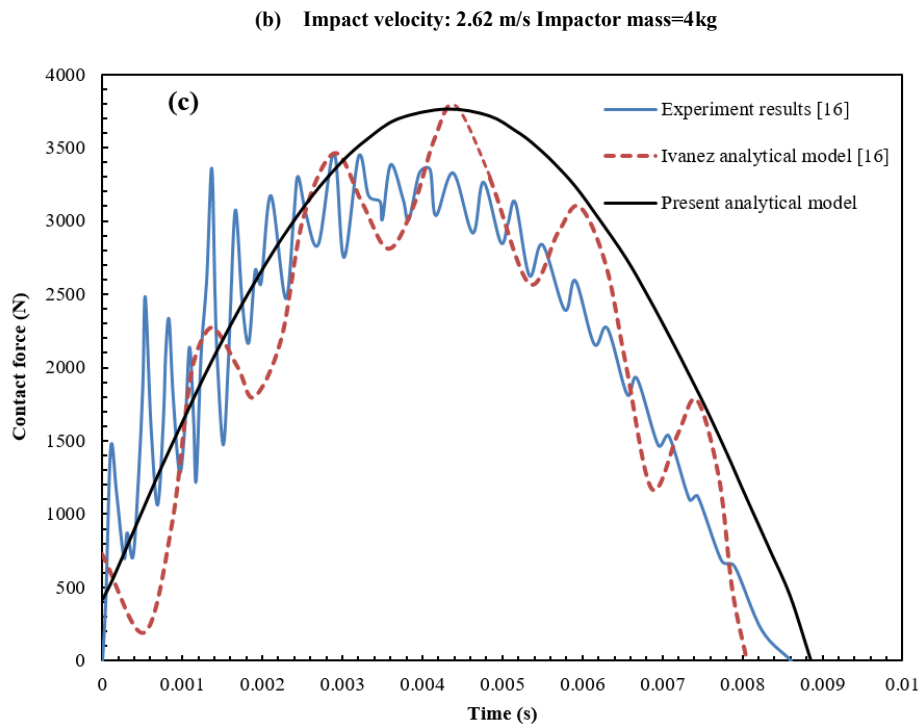
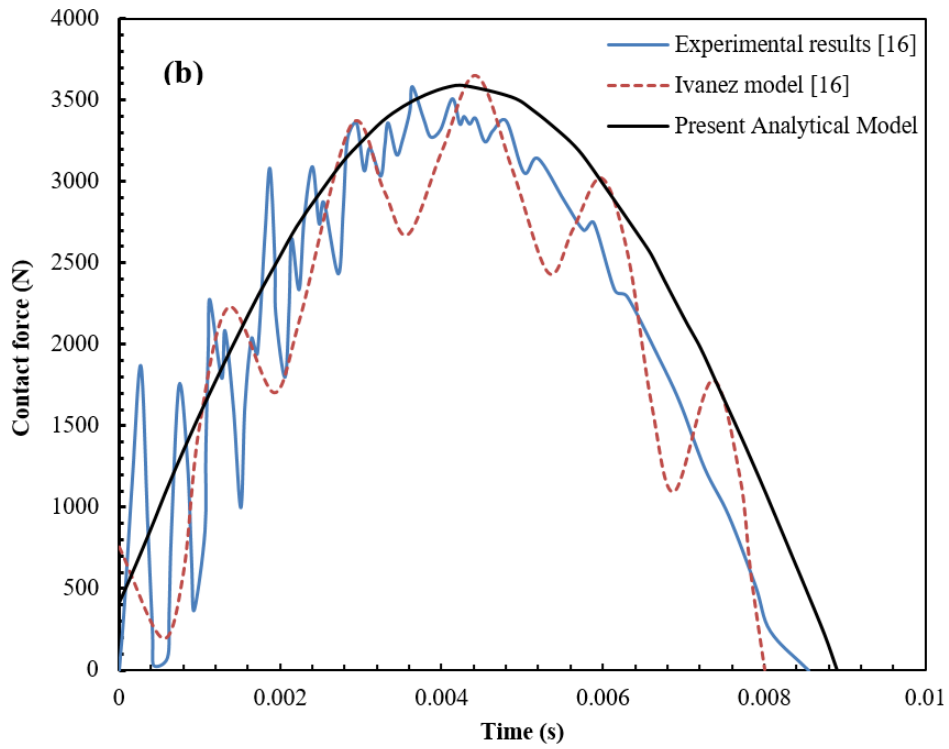


Fig. 11. Experimental and analytical maximum displacement of composite sandwich beam with FOAM core in various impact energies.



(a) Impact velocity: 2.04 m/s Impactor mass=4kg

Fig. 12. Experimental, Ivanez and present analytical model contact force history of a composite sandwich beam with honeycomb core. (Continue)



**Fig. 12. Experimental, Ivanez and present analytical model contact force history of a composite sandwich beam with honeycomb core.**

**Table 3. Comparison of maximum contact force between the new analytical model and experimental [16] results.**

| Impact velocity (m/s) | maximum contact force (kN) |                      | Diff % |
|-----------------------|----------------------------|----------------------|--------|
|                       | Experimental [16]          | New analytical model |        |
| 2.04                  | 2671.20                    | 2792.03              | 4.52   |
| 2.62                  | 3587.04                    | 3587.12              | 0.003  |
| 2.77                  | 3482.10                    | 3768.71              | 8.23   |

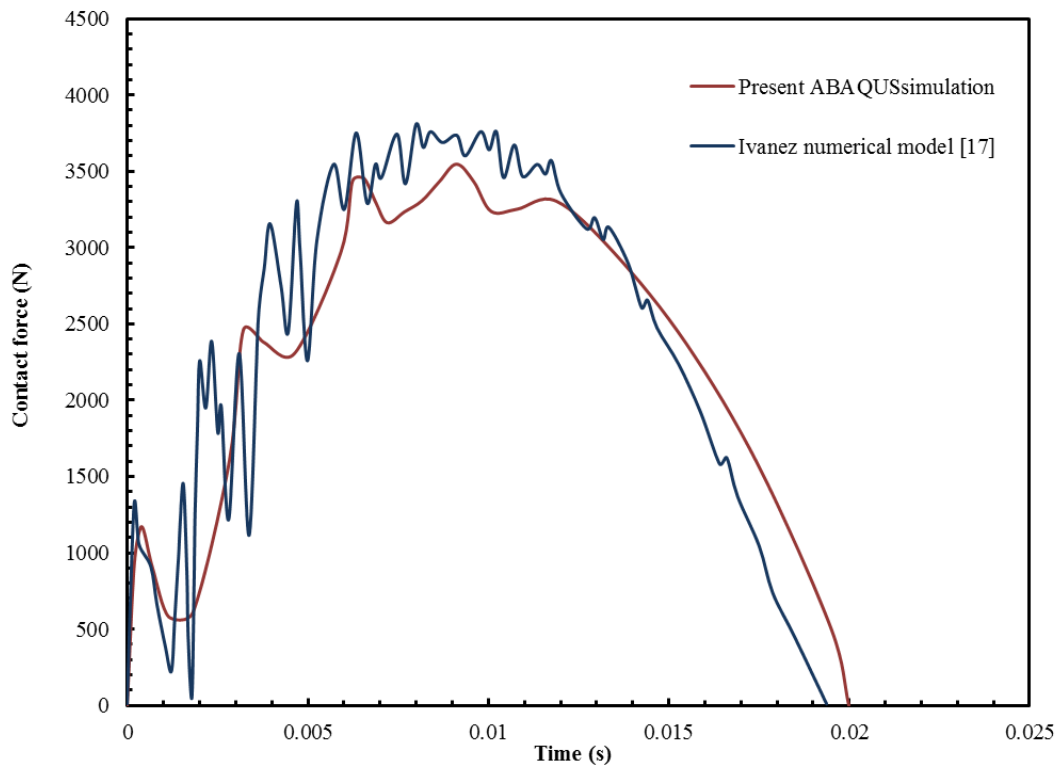


**Fig. 13. Comparison of FE simulation and Ivanez numerical model for contact force history in sandwich beam with FOAM core at impact velocity 3m/s**

**Table 4. Comparison of experimental and analytical contact duration**

| Impact velocity (m/s) | Contact duration (ms)     |                  | Diff % |
|-----------------------|---------------------------|------------------|--------|
|                       | Experimental results [16] | Analytical model |        |
| 2.04                  | 8.96                      | 8.85             | 1.19   |
| 2.62                  | 8.56                      | 8.91             | 2.62   |
| 2.77                  | 8.58                      | 8.86             | 3.22   |

foam. However, in Ivanez’s numerical model [17], the Hou Damage criteria for composite face sheets were applied. The coefficients of mechanical properties in this model, chosen for composite face sheets and foam core, were selected from Ivanez’s study [17].

In Figs. 14 and 15, the contact force and deflection of top face-sheet histories predicted by the new model were compared with the ABAQUS simulation. The results show that, at the same impact energy, lowering the impactor mass and raising the impact velocity have little effect on the maximum contact force and maximum deflection of the sandwich beam, but the contact duration is significantly reduced.

**5- Conclusions**

This paper presented a modified analytical solution for low velocity impact response of simply supported cross-ply composite sandwich beams by using the two degrees of freedom mass-spring model. In this model, based on the small local indentations and indentations more than the top face -sheet’s height, two different equations for computing the contact force, were derived.

The results of the analytical model are compared with two experimental studies: (1) faces-sheets made from E-glass fibers and polyester resin AROPOL FS6902 and a PVC foam core; (2) a 3003 alloy hexagonal aluminum honeycomb core surrounded by two face-sheets composites of carbon fiber and epoxy resin is used.

According to the analytical model results, we can draw the following conclusions:

The contact fore history, maximum contact force, and maximum displacement of composite sandwich beam with FOAM core have good agreement with experimental results at different impact energies.

The contact force history of composite sandwich beam with honeycomb core has good consistency with experimental results at different impact energies.

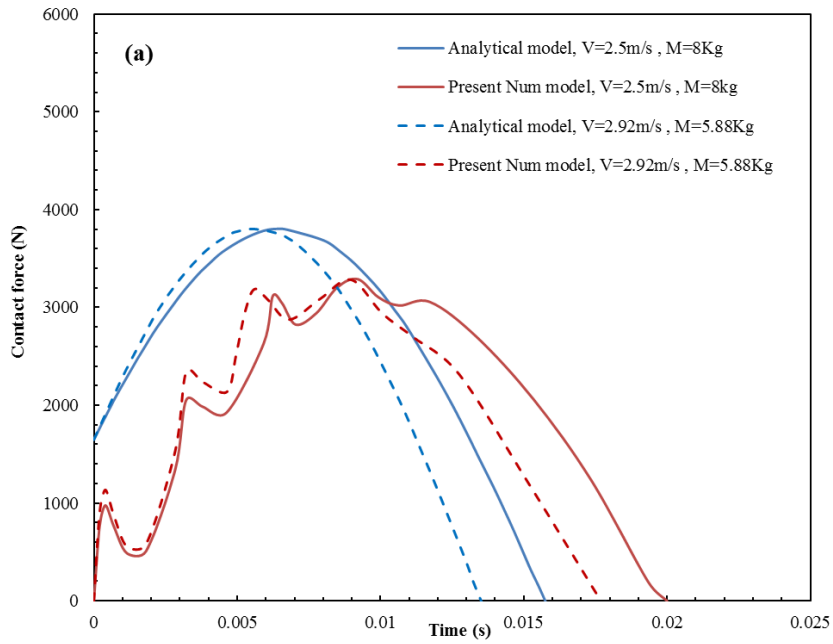
The contact force and top face sheet deflection histories predicted by the analytical model have an acceptable

agreement with the Finite Element Method (FEM) ABAQUS simulation of composite sandwich beam with FOAM core at different impact energies.

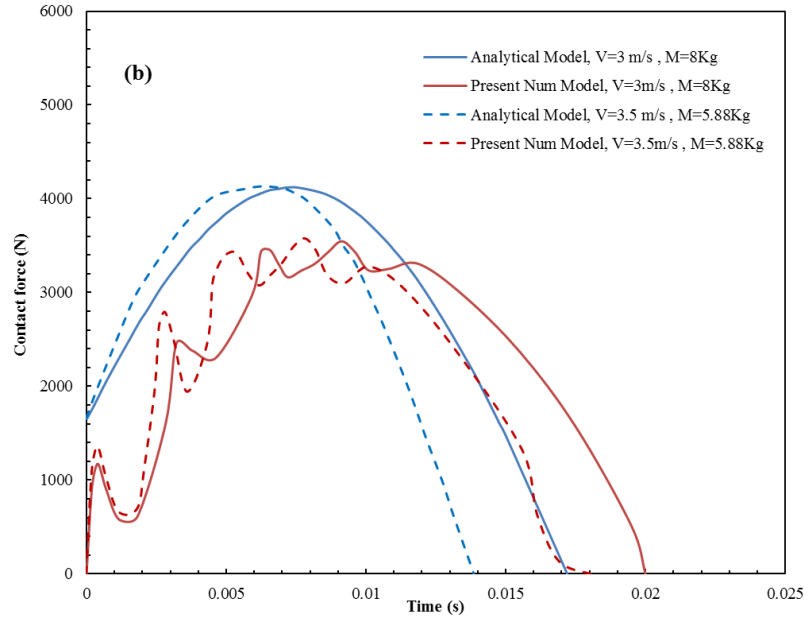
The results show that, at the same impact energy, by decreasing the impactor mass and increasing the impact velocity, the contact duration declines, while the maximum contact force and maximum deflection of the sandwich beam are almost constant.

**Notation**

- $a$  contact radius
- $A_{ij}$  Extensional stiffness matrix of laminate
- $b$  Beam’s width
- $D$  Work due to crushing core
- $D_{ij}$  Bending stiffness matrix of laminate
- $E_{11}$  Longitudinal stiffness of face sheets
- $E_{22}$  Transverse stiffness of face sheets
- $E_c$  Young’s Modulus of the core
- $(EI)_{eq}$  equivalent flexural rigidity of the sandwich beam
- $F_{(t)}$  Contact force
- $G_c$  Core’s in-plane shear modulus
- $G_{12}$  Face sheet’s in-plane shear modulus
- $(GA)_{eq}$  equivalent shear rigidity of the sandwich beam
- $h$  Face sheet’s height
- $h_c$  Core’s height
- $K_g$  global stiffness
- $K_L$  top face sheet stiffness
- $L$  Beam’s length
- $m_f$  equivalent effective mass of face sheet
- $m_s$  equivalent effective mass of sandwich beam

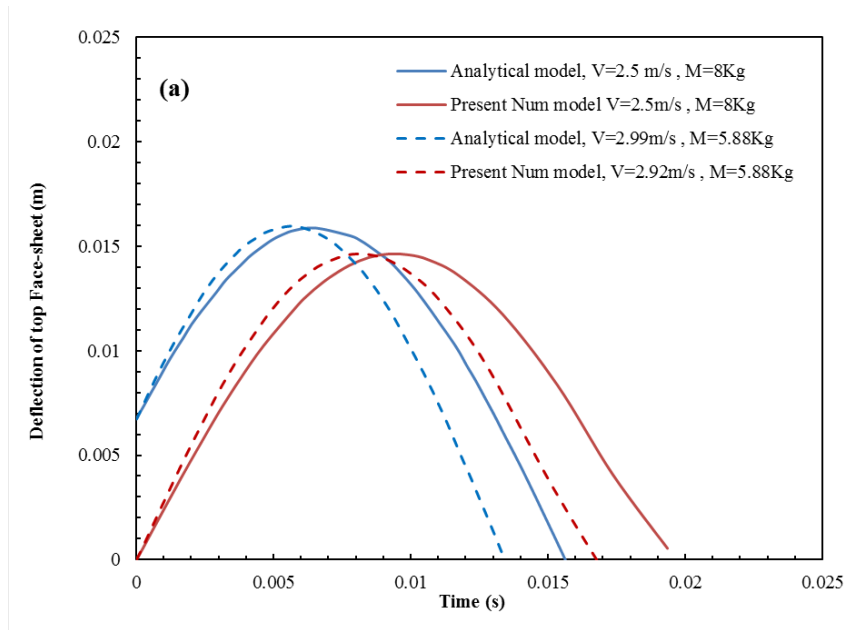


(a) Impact energy: 25J

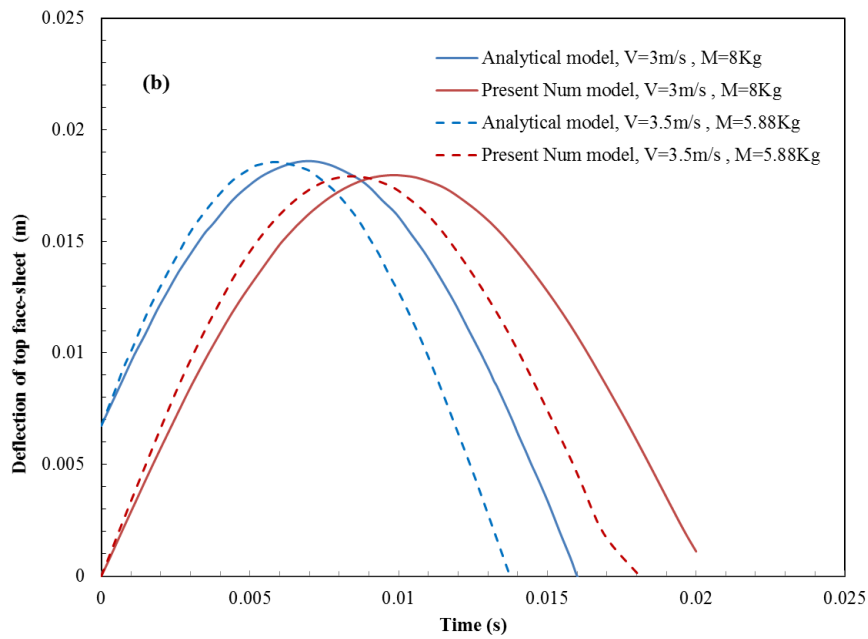


(b) Impact energy: 36J

Fig. 14. Analytical and FE simulation for contact force history in foam based sandwich beam with same impact energy but different impactor mass and velocity.



(a) Impact energy: 25J



(b) Impact energy: 36J

Fig. 15. Analytical and FE simulation for top face sheet deflection history in foam based sandwich beam with same impact energy but different impactor mass.

|                |   |
|----------------|---|
| $M_0$          | Striker's mass                              |
| $P$            | Indentation force                           |
| $q$            | Static core crushing strength               |
| $q_d$          | Dynamic core crushing strength              |
| $Q_d$          | Dynamic core crushing load                  |
| $R$            | Striker's radius                            |
| $U$            | Elastic strain energy                       |
| $V$            | Work done by indentation force              |
| $V_0$          | Impact velocity                             |
| $w(x)$         | Displacement profile of the face sheet      |
| $w_t$          | Top face sheet deflection                   |
| $\delta$       | Local deformation                           |
| $\dot{\delta}$ | Velocity of top face sheet                  |
| $\Delta$       | Global deformation                          |
| $\dot{\Delta}$ | Velocity of sandwich beam                   |
| $\Delta_b$     | Deformation of sandwich beam due to bending |
| $\Delta_s$     | Deformation of sandwich beam due to shear   |
| $\nu_c$        | Poisson's ratio of face sheet               |
| $\nu_{12}$     | Poisson's ratio of core                     |
| $\xi$          | Deformation zone's length                   |
| $\Pi$          | Total potential energy                      |
| $\rho_f$       | Density of top face sheet                   |
| $\rho_c$       | Density of core                             |
| $\rho_s$       | Density of sandwich beam                    |

## References

- [1] J.R. Vinson, Sandwich structures, *Applied Mechanics Reviews*, 54(3) (2001) 201-214.
- [2] E.B. Inés Ivañez, Sonia Sanchez-Saez, Analytical study of the low-velocity impact response of composite sandwich beams, *Composite Structures*, 111 (2014) 459-467.
- [3] K.S.P. Michell S. Hoo Fatt, Dynamic models for low velocity impact damage of composite sandwich panels – Part A: Deformation, *Composite Structures*, 52(3) (2001) 335-351.
- [4] S. Abrate, Impact on laminated composites, *Recent Advances, Applied Mechanics Reviews*, 47(11) (1994) 517-544.
- [5] S. Abrate, Localized impact on sandwich structures with laminated facing, *Applied Mechanics Reviews*, 50(20) (1997) 68-82.
- [6] S. Abrate, Modeling of impacts on composite structures Impact on laminated composite materials, *Composite Structures*, 51(2) (2001) 129-138.
- [7] J.L. Abot, Daniel, I. M., & Gdoutos, E. E., Contact law for composite sandwich beams, *J Sandwich Struct Mate.*, 4(2) (2002) 157-173.
- [8] T.M. McCormack, Miller, R., Kesler, Failure of sandwich beams with metallic foam cores, *Journal of Sandwich Structure Materials*, 4(2) (2002) 157-173.
- [9] L.J.-J. Schubel P. M., Daniel I.M., , Low-velocity impact behavior of composite sandwich panels, *Compos. Part A.*, 36(10) (2005) 1389-1396.
- [10] W.J. E., Response mechanisms in the impact of graphite/epoxy honeycomb sandwich panels, MIT, 1991.
- [11] C.L. Wu, Sun, C. T. , Low velocity impact damages in composite sandwich beams, *Composite Structures*, 34 (1996) 1.
- [12] T. Anderson, Madenci, E., Experimental investigation of low-velocity impact characteristics of sandwich composites, *Composite Structures*, 50(3) (2000) 239-247.
- [13] C.C. Foo, Chai, G.B., L.K. Seah, A model to predict low-velocity impact response and damage in sandwich composites, *Composite Science Technology*, 68(6) (2008) 1348-1356.
- [14] U. Icardi, Ferrero, L., Impact analysis of sandwich composites based on a refined plate element with strain energy updating, *Composite Structures*, 89(1) (2009) 35-51.
- [15] M. Meo, Morris, A. J., Vignjevic, R., & Marengo, G. , Numerical simulations of low velocity impact on an aircraft sandwich panel., *Composite Structures*, 62(3) (2003) 353-360.
- [16] S.-S.S. Ivañez I, Numerical modelling of the low-velocity impact response of composite sandwich beams with honeycomb core, *Composite Structures*, 106 (2013) 716-723.
- [17] S.C. Ivañez I, Sanchez-Saez S., FEM analysis of dynamic flexural behavior of composite sandwich beams with foam core, *composite Structures*, 92(9) 2285–2291.
- [18] T.A. Anderson., An investigation of SDOF models for large mass impact on sandwich composites, *Composites: Part B*, 36(2) (2005) 135-142.
- [19] R. Olsson, Engineering Method for prediction of impact response and damage in sandwich panels, *Journal of Sandwich Structure Materials*, 4(1) (2002) 3-29.
- [20] D.W. Zhou, & Stronge, W. J., Low velocity impact denting of HSSA lightweight sandwich panel., *International Journal of Mechanical Science*, 48(10) (2006) 1031-1045.
- [21] M.A. Hazizan, & Cantwell, W. J., The low velocity impact response of foam-based sandwich structures, *Composites: Part B*, 33(3) (2002) 193-204.
- [22] M.A. Hazizan, & Cantwell, W. J., The low velocity impact response of an aluminum honeycomb sandwich structure., *Composites: Part B*, 34(8) (2003).
- [23] R.S. Hasebe, & Sun, C. T. , Performance of sandwich structure with composite reinforced core, *Journal of Sandwich Structure Materials*, 2(1) (2000) 75-100.
- [24] C. Chen, Harte, A. M., & Fleck, N. A. . I., The plastic collapse of sandwich beams with a metallic foam core, *Int. J Mech. Sci.* , 43(6) (2001) 1483-1506.
- [25] H.F.M. Türk MH, Localized damage response of

- composite sandwich plates, *Compos Part B*, 30(2) (1999) 157-165.
- [26] M. Meo, Vignjevic, R., & Marengo, G. , The response of honeycomb sandwich panels under low-velocity impact loading, *Int. J Mech. Sci.*, 47(9) (2005) 1301-1325.
- [27] Y. Frostig, and M. Baruch., Buckling of simply-supported sandwich beams with transversely flexible core—a high order theory, *J. Eng. Mech.*, 119 (1993) 955-972.
- [28] Y. Frostig, Bending of sandwich beams with transversely flexible core and transverse diaphragms, *J. Eng. Mech. Div., ASCE.* , 119(5) (1993) 955-972.
- [29] Y. Frostig, & Shenhar, Y. , High-order bending of sandwich beams with a transversely flexible core and unsymmetrical laminated composite skins, *Compos. Eng.* , 5(4) (1995) 405-444.
- [30] Z. Xie, Zheng, Z., & Yu, J. , Localized indentation of sandwich beam with metallic foam core, *Journal of Sandwich Structure Materials*, 14(2) (2011) 197-210.
- [31] P. Navarro, Abrate, S., Aubry, J., Marguet, S., & Ferrero, J. F. , Analytical modeling of indentation of composite sandwich beam., *Composite Structures*, 100 (2013) 79-88.
- [32] A.L. Dobyns, Analysis of simply-supported orthotropic plates subject to static and dynamic loads, *AIAA J* 19(5) (1981) 642-650.
- [33] K.S. Hibbit, ABAQUS/Explicit user's manual Version 6.4.

#### HOW TO CITE THIS ARTICLE

*P. Karvan, S. Feli, Low Velocity Impact Response of Sandwich Beams with Composite Face-Sheets and Foam or Honeycomb Core: Analytical Modeling and Finite Element Simulation, AUT J. Mech Eng., 6(3) (2022) 341-362.*

**DOI:** [10.22060/ajme.2022.20713.6014](https://doi.org/10.22060/ajme.2022.20713.6014)

